

AIR EXCHANGE MECHANISM IN 3-D COMPLEX ARRAY

Klára Jurčáková¹, Štěpán Nosek¹, Zuzana Kluková^{1,2}, Radka Kellnerová¹, Zbyněk Jaňour¹

¹Institute of Thermomechanics, Czech Academy of Sciences, Prague, Czech Republic

²Charles University in Prague, Faculty of Mathematics and Physics, Prague, Czech Republic

Abstract: In this paper, a wind-tunnel study on dispersion of a tracer gas emitted from a ground-level line source positioned within complex obstacle arrays is presented. The models consisted of courtyard buildings blocks with pitched roofs and of uniform and non-uniform heights. Tracer exchange between the street canyon cavities and surrounding flow was studied by simultaneous point measurement of flow and tracer concentration. While there was found a significant impact of the roof-height variability on the tracer exchange rate from the canyon in the case of wind approaching perpendicularly to the along-canyon axis, in the case of the oblique wind the impact was insignificant.

Key words: wind tunnel, street canyon, pollution flux measurement.

INTRODUCTION

Air pollution in cities is still a major problem with respect to public health. Small but numerous pollution sources (e.g., vehicles, local heating) are releasing harmful substances within urban canopy comprising array of buildings of complex geometries. In our previous studies (Nosek et al., 2016, and Nosek et al. 2017) idealized 3-D urban arrays were tested in the wind tunnel to assess the pollution ventilation mechanism of individual street canyons in more complex arrangements than usual 2-D set-ups with uniform flat roofs. Also the oblique wind direction (45°) was tested to show the behavior in more realistic configuration than the strictly perpendicular wind direction. The paper sum up previously published papers (Nosek et al., 2016 and Nosek et al., 2017).

EXPERIMENTAL SETUP

The experiments were conducted under neutrally stratified conditions in an open low-speed wind tunnel. Atmospheric boundary layer (ABL) was simulated above wind-tunnel floor using turbulence generators and roughness elements in the scale of 1:400. Wind-tunnel freestream velocity was $U_0 = 6.2$ m/s. Parameters of created ABL were: roughness length, $z_0 = 1.87$ m; displacement height, $d_0 = 3$ m; and normalized friction velocity, $u^*/U_0 = 0.07$; all at full scale. Created boundary layer corresponded to the flow above very rough terrain.

To study the effect of urban array three-dimensionality and wind directionality on pollutant transport from traffic while keeping the configuration as simple as possible, we designed two urban array models (Fig. 1). Both idealized models were formed by 384 buildings, which created evenly spaced 8 x 4 courtyard-type blocks (each consisting of 12 buildings) of constant length ($L = 300$ mm) and width ($B_B = 150$ mm). The difference between the models consisted of the heights of the pitched roofs. While the reference urban model (A1, Fig. 1a) had a constant roof height ($H = 62.5$ mm, i.e., 25 m at full scale), the second urban model (A2, Fig. 1b) had arbitrarily distributed roof heights among the buildings (Fig. 1b). The three types of buildings with different roof-heights ($z/H = 0.8, 1,$ and 1.2 , respectively, Fig. 1d) had the relative occurrence 28%, 44%, and 28%, respectively, in order to keep the mean building height the same for both the models. Also plan and frontal areas matched for both the models, but every street has unique building-height variability. Two investigated street canyons were labeled as L and R (Fig. 1b). We simulated the pollution from traffic by means of a ground-level line source that emitted the tracer gas

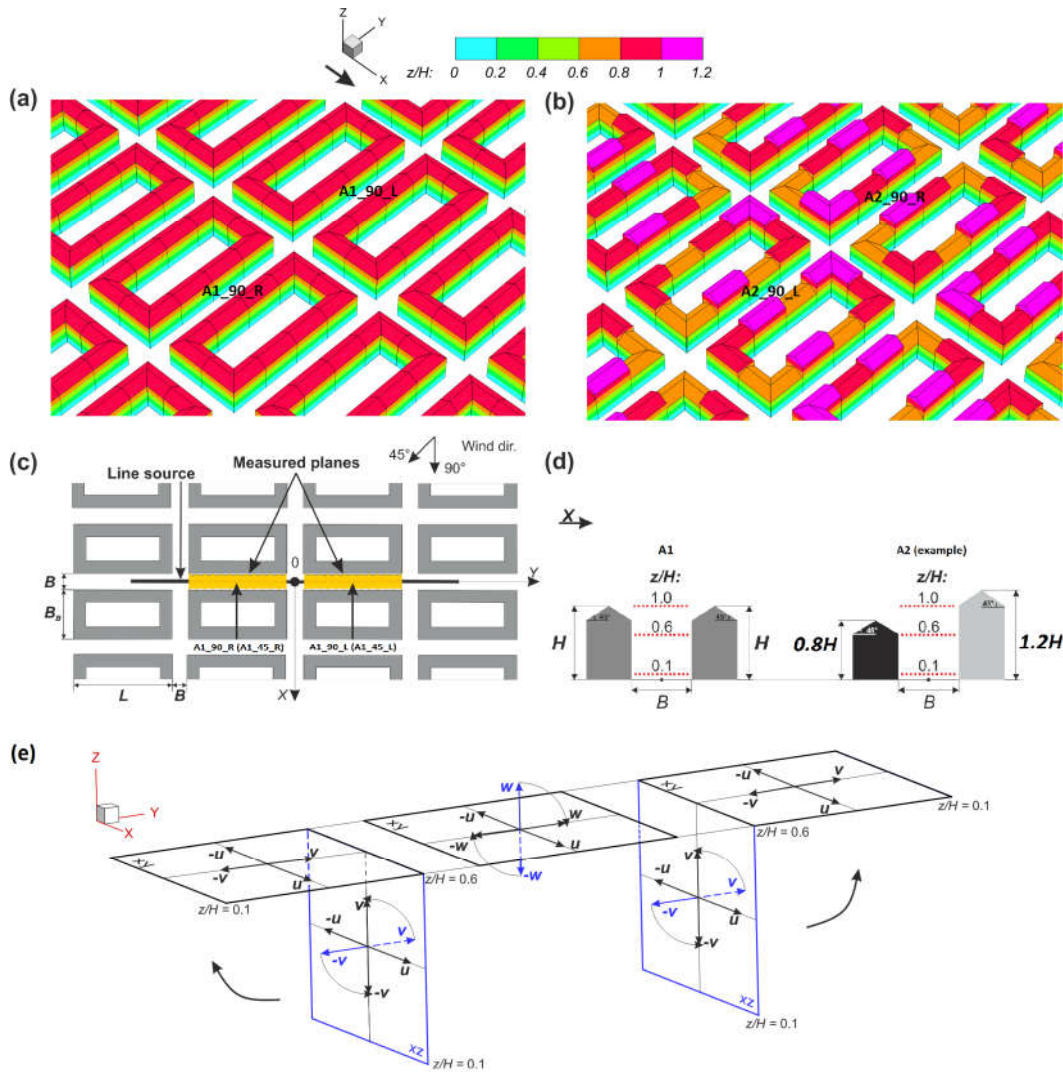


Figure 1. Schemas of the model: **a)** model A1; **b)** model A2; **c)** top view of the model with courtyard blocks and the line source in the middle of the investigated street canyon; **d)** side view of the A1 model (left) and example of A2 model (right); **e)** the transformation of the coordinates and velocity vectors. Adapted from Nosek et al. (2016) and Nosek et al. (2017).

(ethane) homogeneously and it run through four consequent street canyons (Fig. 1c). For both urban-array models we simulated two wind directions: perpendicular and oblique (45°) to the line source.

Simultaneous point measurements of two velocity components and the tracer concentration using a Dantec Laser Doppler Anemometry (LDA) probe and a probe of a Cambustion HFR400 fast-response flame ionization detector (FFID) was used for the measurement of the pollutant transport. The LDA and FFID probes were assembled together on a 3D traverser system approx. 2 mm aside. Due to the length (200 mm) of the FFID sample tube, the mean delay in the physical sampling time relative to that of LDA was approximately 12 ms, which was used for the synchronization between the velocity and concentration time series.

Fig. 1c shows the positions of the horizontal measurement planes, which were measured at the height of $0.6H$ to ensure that this plane is below the building eave for all building heights (see the lowest building in Fig. 1d). The vertical planes were measured at the street canyon ends. Tracer fluxes were computed

from the velocity component normal to the planes (the vertical component w for the top and the lateral component v for the canyon ends) and the concentration. All three planes formed a box, which enables us to perform the tracer flux balance analysis for both the uniform and the non-uniform canyons. Further details regarding the experimental set-up and conditions are reported in Nosek et al. (2016) and Nosek et al. (2017).

RESULTS

To be able to show values measured at all planes together the transformation of coordinates was used. For this, we used the transformation of the lateral planes (xz , labelled blue in Fig. 1e) to the horizontal plane (xy , labelled black in Fig. 1e) by rotating by an angle of 90° and -90° , respectively. Hence folding their bottom ($z/H = 0.1$) up to the horizontal plane at the dimensionless height $z/H = 0.6$. For the mean total tracer flux fields we used the following dimensionless form: $\langle c^*w \rangle / U_0$ for the total vertical and $\langle c^*v \rangle / U_0$, for the total lateral tracer fluxes, where w and v are the instantaneous vertical and lateral velocity components, respectively, and c^* is the instantaneous dimensionless concentration computed as

$$c^* = \frac{cL_sU_0H}{Q} \quad (1)$$

where c is the measured instantaneous volume concentration, L_s is the length of the line source, and Q is the tracer volume flow rate from the line source. The angular brackets for $\langle c^*w \rangle / U_0$ represent the time averaging of the measured 120 s long time series at the sampling rate of 500 Hz.

The mean dimensionless tracer flux fields are presented in Fig. 2 (contour plots created by interpolating between 150 measurement points), for both simulated wind directions. We computed the surface integral of the normal tracer flux for each plane presented in Fig. 2 in order to perform the preliminary analysis of the tracer flux balance of each of the canyon. The resulting relative tracer fluxes are shown in Fig. 3, where $E_{\text{lat_R}}$ is the relative flux through the right (in the sense of the flow direction) street canyon end, $E_{\text{lat_L}}$ through the left end, E_{top} through the horizontal plane at $0.6H$, and E_{tot} is the flux sum for the whole street-canyon box. An ideal pollution flux balance should sum up to the flux from the source, Q (i.e. to 1 in dimensionless representation). Our balances differed from 1 significantly because of the unmeasured fluxes close to walls. Due to the measurement constraints nearby the street-canyon walls and floor, the investigated area covered only 77% of the total area. We are missing fluxes near the walls and at the bottom, where the velocity is decaying, but the concentrations values are high and potential tracer flux non-negligible.

Within the uncertainty of the computed pollution fluxes (15%) there are insignificant differences between the relative pollution fluxes for the case of the oblique wind amongst the investigated canyons (A1-45, A2-45-R, and A2-45-L in Fig. 3). However, both non-uniform street canyons (A2-90-R and A2-90-L in Fig. 3) showed appreciable enhanced vertical transport (hatched columns) compared to the uniform canyon (A1-90) set-up in the case of the perpendicular wind (compare also the mean total pollution flux fields in Figs. 2b and 2c). We are expecting that the additional pollution might be transported to the street canyon from the intersections and then venting upwards through these canyons through their top openings which might be enhanced by the street-canyon roof-height non-uniformity. Indeed, as we described earlier in our work (Nosek et al., 2017), the local step-down building arrangement causes flow convergence behind the higher building and thus entraining air from intersection (which might be polluted in the case of line source longer than the street canyon, and hence represent the traffic through the intersections) and venting it upward. The local step-up arrangement causes flow divergence in front of the higher building (entrain the high-momentum flow to the street canyon cavity) and enhanced the air exchange with the above-roof flow. These flow enhancements are amplified also by the roof-height non-uniformities along the entire intersections as was also observed in the field experiments (Pol et al. 2008, Balogun et al. 2010). This issue is a part of our ongoing research and will be published soon.

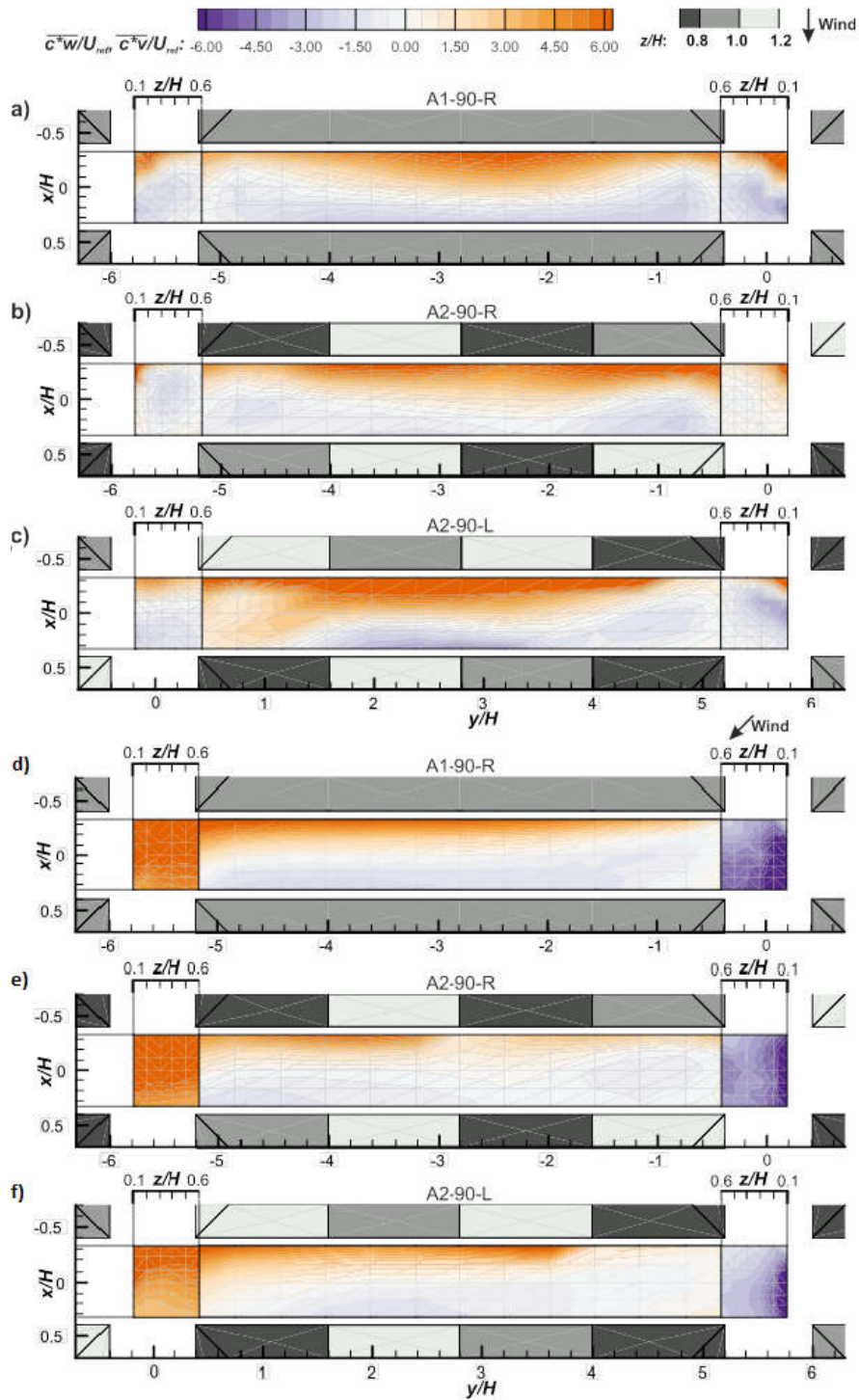


Figure 2. Mean dimensionless total tracer flux fields for the **a-c)** normal and **d-f)** oblique wind direction. **a)** Uniform canyon (A1-90-R), and the non-uniform **b)** right (A2-90-R) and **c)** left (A2-90-L) street canyon; **d)** uniform canyon (A1-90-R), and the non-uniform **e)** right (A2-90-R) and **f)** left (A2-90-L) street canyon. The positive (orange) contour fields represent the outgoing flux while the negative (violet) contour fields represent the incoming flux to the street-canyon.

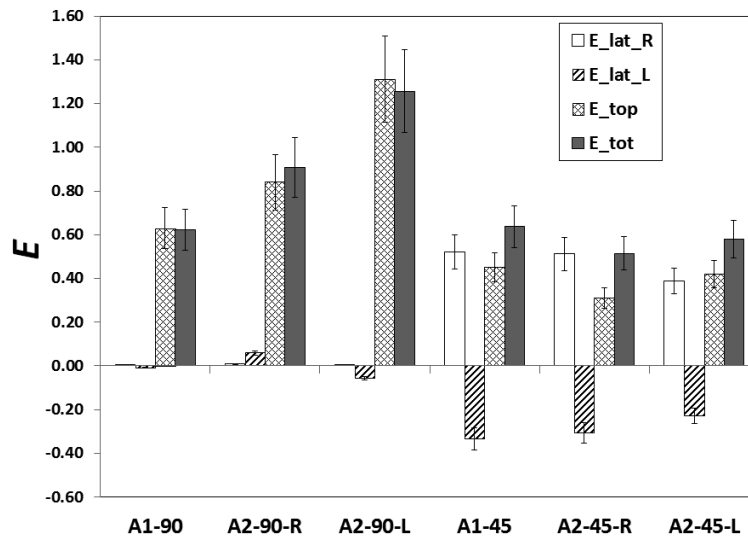


Figure 3. Balances of the relative tracer fluxes through the measured planes. The positive values of E represents outgoing relative tracer fluxes, the negative values ingoing fluxes. The error bars represent the estimated relative error of the computed relative total tracer fluxes (15%).

CONCLUSION

Roof-height variability showed to be very important for the street-canyon ventilation of traffic pollution. The local step-down building arrangement causes flow convergence and thus entraining air from intersection (which might be polluted in the case of traffic line going through the intersection) and venting it upward. The local step-up arrangement causes flow divergence and enhances the air exchange with the above-roof flow. Owing to only 77% of the total street-canyons' opening areas covered by the measurement, we were unable to obtain the entire flux balance because of the unmeasured possible fluxes close to the canyons' walls and floor. This issue is a part of our ongoing research where such measurements are currently tested.

ACKNOWLEDGEMENT

This work was supported by the Czech Science Foundation GACR (project GAP15-18964S) and the institutional support RVO: 61388998.

REFERENCES

- Balogun, A. A., Tomlin, A. S., Wood, C. R., Barlow, J. F., Belcher, S. E., Smalley, R. J., Lingard, J. J. N., Arnold, S. J., Dobre, A., Robins, A. G., Martin, D., Shallcross, D. E., 2010. In-street wind direction variability in the vicinity of a busy intersection in central London. *Boundary-Layer Meteorol.* 136 (3), 489–513.
- Nosek, Š., Kukačka, L., Kellnerová, R., Jurčáková, K., Jaňour, Z., 2016. Ventilation processes in a three-dimensional street canyon. *Boundary-Layer Meteorol.* (159), 259–284.
- Nosek, Š., Kukačka, L., Jurčáková, K., Kellnerová, R., Jaňour, Z., 2017. Impact of roof height non-uniformity on pollutant transport between a street canyon and intersections. *Environmental Pollution* (227), 125–138.
- Pol, S. U., Brown, M. J., 2008. Flow Patterns at the Ends of a Street Canyon: Measurements from the Joint Urban 2003 Field Experiment. *J. Appl. Meteorol. Climatol.* 47 (5), 1413–1426.